nature ecology & evolution

ARTICLES

https://doi.org/10.1038/s41559-018-0549-8

Multi-environment fitness landscapes of a tRNA gene

Chuan Li[1,2] and Jianzhi Zhang[1*]

A fitness landscape (FL) describes the genotype–fitness relationship in a given environment. To explain and predict evolution, it is imperative to measure the FL in multiple environments because the natural environment changes frequently. Using a high-throughput method that combines precise gene replacement with next-generation sequencing, we determine the in vivo FL of a yeast tRNA gene comprising over 23,000 genotypes in four environments. Although genotype-by-environment interaction is abundantly detected, its pattern is so simple that we can transform an existing FL to that in a new environment with fitness measures of only a few genotypes in the new environment. Under each environment, we observe prevalent, negatively biased epistasis between mutations. Epistasis-by-environment interaction is also prevalent, but trends in epistasis difference between environments are predictable. Our study thus reveals simple rules underlying seemingly complex FLs, opening the door to understanding and predicting FLs in general.

The fitness landscape (FL) of a gene in a given environment maps each mutational variant of the gene to the fitness of the organism carrying the variant. FLs help to explain as well as predict evolutionary trajectories, and are therefore of fundamental biological importance[1]. Because fitness is expected to vary by environment, which frequently changes in nature, characterizing FLs in multiple environments not only makes evolutionary explanations and predictions more relevant and accurate, but under certain circumstances also offers insights that are otherwise impossible to gain. For example, a gene that seems harmful to an organism in one environment is nonetheless retained in its genome because it is beneficial in other environments[2]. Two alleles at a locus may be respectively favoured in two environments, resulting in a stable genetic polymorphism if the population switches sufficiently frequently between these environments[3,4]. A population trapped at a suboptimal local fitness peak under one environment may escape upon an environmental shift, even if the environment later shifts back[5,6]. Differences in the FL between two environments may also lead to ecological speciation[7]. Nevertheless, due to the huge genotype space (4^n genotypes for a gene with n nucleotides), even the characterization of a small fraction of the FL of a gene under one environment was a formidable challenge until recently[8–13]. As a result, past quantifications of FLs typically probed only one environment. Adopting a recently developed high-throughput method[9] with minor modifications, we mapped the in vivo FL of a tRNA gene in four environments to study the environmental impact on FLs. Of particular interest were genotype-by-environment (G×E) interactions and epistasis-by-environment (G×G×E) interactions. In humans, G×E has been implicated in numerous diseases such as cancer and mental disorders[14,15]. Epistasis, or interaction between mutations (G×G), has multiple important functional and evolutionary implications[16] and is known to vary among environments[17–22]. Because the method employed can measure the fitness of tens of thousands of genotypes[9], the collected data permit the quantification of G×E and G×G×E at an unprecedentedly large scale, providing opportunities for identifying general principles of these interactions.

Results

Mapping multi-environment FLs of a tRNA gene. $tRNA^{Arg}_{CCU}$ is a transfer RNA that uses its anticodon 5′-CCU-3′ to bind to the arginine codon AGG in translation. It is encoded by a single-copy gene (*HSX1*) in the budding yeast *Saccharomyces cerevisiae*. Deleting this gene is non-lethal because $tRNA^{Arg}_{UCU}$—another tRNA for arginine—can wobble-pair with AGG. We synthesized the 72-nucleotide $tRNA^{Arg}_{CCU}$ gene with a 3% per-site mutation rate (1% to each alternative nucleotide) at 69 sites; the remaining 3 sites were kept invariant for technical reasons[9] (Fig. 1; see Methods). This mutation rate was chosen to maximize the representation of genotypes carrying two mutations for the purpose of studying epistasis between mutations (see Methods). We constructed a library of more than 100,000 yeast strains, each carrying a $tRNA^{Arg}_{CCU}$ gene variant at its native genomic location. Three to five parallel competitions of this strain pool were conducted in each of four environments: 30 °C in the rich medium YPD (hereafter Env_{30}), 23 °C in YPD (Env_{23}), 37 °C in YPD (Env_{37}) and 30 °C in YPD with 3% dimethyl sulfoxide (DMSO) added (Env_{DMSO}) (Fig. 1). Among them, Env_{30} is the optimal growth condition for the wild-type yeast strain used, with the other environments imposing cold, heat and oxidative stresses[23], respectively. The selection of these four environments was based on previous studies showing that tRNA folding and decay are temperature dependent[24–26] and RNA structure and function are affected by DMSO[27].

The wild-type yeast growth rates (GR) in these four environments were in the order $GR(Env_{30}) > GR(Env_{DMSO}) > GR(Env_{37}) > GR(Env_{23})$, while the gene importance (GI) to growth, measured by the fractional reduction in growth rate caused by deleting the tRNA gene, was in the order $GI(Env_{37}) > GI(Env_{DMSO}) > GI(Env_{30}) > GI(Env_{23})$ (Supplementary Fig. 1). The $tRNA^{Arg}_{CCU}$ gene is therefore more important to cell growth at higher temperatures, probably because the probability that $tRNA^{Arg}_{UCU}$ is correctly folded decreases with temperature, reducing its ability to compensate for the loss of the $tRNA^{Arg}_{CCU}$ gene.

After the competition, the $tRNA^{Arg}_{CCU}$ gene amplicons from each replicate competition (T_1) under each environment, as well as those

[1]Department of Ecology and Evolutionary Biology, University of Michigan, Ann Arbor, MI, USA. [2]Present address: Department of Biology, Stanford University, Stanford, CA, USA. *e-mail: jianzhi@umich.edu

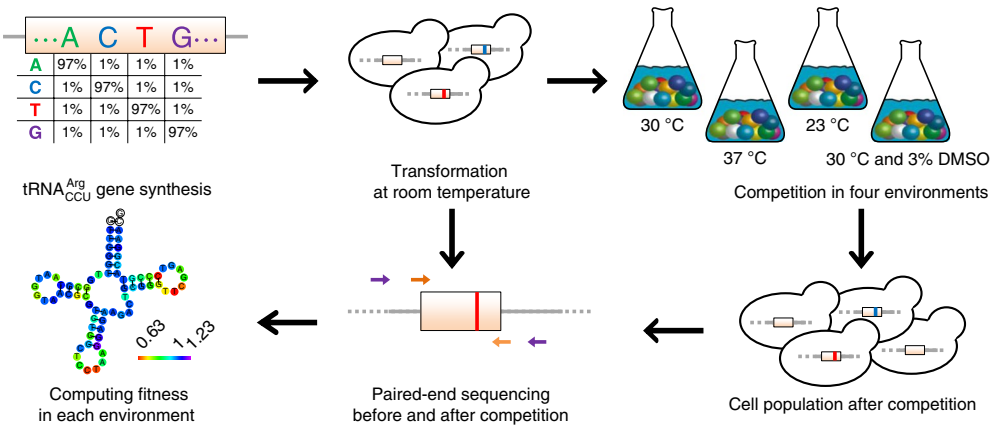

Fig. 1 | Determining the FL of the yeast tRNA$^{Arg}_{CCU}$ gene in multiple environments. Chemically synthesized tRNA$^{Arg}_{CCU}$ gene variants were incorporated at the native genomic locus of the gene. Transformation was conducted at room temperature to ensure comparatively equal representation of mutant strains. The tRNA variant-carrying cells competed for ~13 generations in each environment at the log phase, and the tRNA gene variants were sequenced before and after the competition. The fitness of each tRNA$^{Arg}_{CCU}$ genotype relative to the wild-type was calculated from the relative frequency change of paired-end sequencing reads covering the tRNA gene variant during competition.

from the common starting population (T_0; with two technical repeats), were sequenced by 125-nucleotide paired-end Illumina sequencing (Fig. 1). The sequences provided the tRNA$^{Arg}_{CCU}$ genotype as well as genotype frequency information. A total of 881 million read pairs were generated. Read numbers per genotype were highly correlated between technical repeats (Pearson's correlation $r=0.994$; Supplementary Fig. 2a) and between biological replicates ($r=0.9911$–0.9999; Supplementary Fig. 2b). The technical repeats were combined in subsequent analyses. The fitness of each genotype relative to the wild-type (fitness hereafter) in an environment was estimated using the genotype frequencies at T_0 and T_1 as well as the number of wild-type generations in the competition (see Methods). We analysed 23,284 genotypes with read counts ≥100 at T_0. Because the tRNA$^{Arg}_{CCU}$ gene is non-essential, mutations in the gene were unlikely to be lethal. When an estimated fitness was <0.5 (probably due to stochasticity), we set it at 0.5, meaning that the genotype had no growth[9].

G×E is pervasive. Previously, we reported the FL of the yeast tRNA$^{Arg}_{CCU}$ gene in Env$_{37}$ and its reliability, consistency with evolutionary data and potential mechanistic basis[9]. Here, with the FL data in four environments, we focus on the impact of the environment on the FL rather than describing the FL under each environment. Specifically, we studied whether the same mutation has different fitness effects in different environments, formally known as genotype-by-environment interaction[28] (G×E) in fitness (Fig. 2a). Under the null hypothesis of no G×E, the fitness effect of a mutation is environment independent, and hence the mutant fitness distribution should be identical across environments. In stark contrast with this null expectation, the mutant fitness distribution differed drastically among each pair of the four environments ($P<10^{-300}$, Kolmogorov–Smirnov test; Fig. 2b), suggesting pervasive G×E in our data. Mean mutant fitness ($\overline{F}$) was in the order $\overline{F}(\text{Env}_{23})>\overline{F}(\text{Env}_{30})>\overline{F}(\text{Env}_{\text{DMSO}})>\overline{F}(\text{Env}_{37})$—exactly opposite to the aforementioned order of *GI* in the four environments. That is, mean mutant fitness decreased as gene importance in the environment increased. Although testing G×E for individual genotypes had a much-reduced statistical power, a substantial fraction showed significantly different fitness values between environments (nominal $P<0.05$, *t*-test; lower left triangle in Fig. 2c). This fraction generally increased with the extent of environmental difference that could be gauged (for example, temperature difference). It also increased for genotypes carrying a single point mutation (N1 mutants; upper right triangle in Fig. 2c), owing to their relatively high genotype frequencies in the strain pool that led to relatively high numbers of sequencing reads, which empowered the statistical test. Because only 5% of genotypes were expected by chance to show significantly different fitness values between any pair of environments under the null hypothesis of no G×E, our findings establish the prevalence of G×E. In some studies, G×E is defined by a between-environment variation in the growth rate difference between a genotype and the wild-type[28–31]. Pervasive G×E was also found when growth rate difference instead of relative fitness was used in the definition of G×E (Supplementary Fig. 3; see Methods).

Quantitative relationship in genotype fitness between environments. Despite the abundance of G×E, the fitness of a genotype in one environment exhibited a strong linear correlation with that in another environment ($r=0.78$–0.94; lower left triangle in Fig. 3a), especially for N1 mutants ($r=0.94$–0.99; upper right triangle in Fig. 3a), which generally had more precise fitness estimates than mutants carrying two or more mutations. The correlation was confirmed by individually measuring the fitness of 55 mutants across the four environments on the basis of growth curves ($r=0.85$–0.96; Supplementary Fig. 4).

To more accurately describe the relationship between genotype fitness in two environments, we plotted a local regression (LOESS) of the fitness in Env$_{30}$ (f_{30}) and the fitness in Env$_{23}$ (f_{23}) across all genotypes (Fig. 3b). As expected, the regression goes near the point of ($f_{30}=1$, $f_{23}=1$) because of a large number of genotypes showing similar fitness to the wild-type. The regression suggests that the data can be described approximately by a piecewise linear model of $f_{23}-1=k(f_{30}-1)$, with one slope (k_a) for genotypes of $f_{30}<1$ and a different slope (k_b) for genotypes of $f_{30}>1$ (see Supplementary Table 1 for other environment pairs). In other words, the fitness effect of a mutation in Env$_{23}$ (that is, $f_{23}-1$) is proportional to that in Env$_{30}$ (that is, $f_{30}-1$). We observed a general trend that k_b is closer to 1 than is k_a (that is, $|k_b-1|<|k_a-1|$) across all environment pairs (Fig. 3b and Supplementary Table 1). This pattern may reflect different properties of deleterious and beneficial mutations other than their effect size differences, because the same trend holds even for deleterious and beneficial mutations of comparable fitness effect sizes. We also respectively tested a simple linear model with only one parameter and a

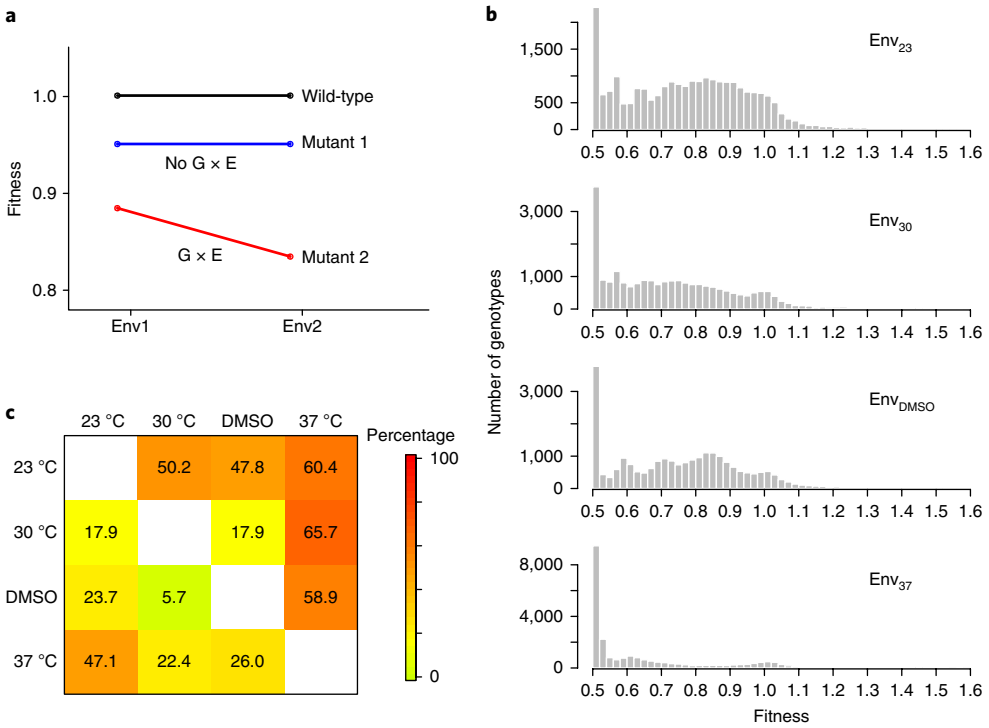

Fig. 2 | Yeast $tRNA^{Arg}_{CCU}$ gene FL in each of the four environments examined. a, Definition of G × E based on mutant fitness relative to the wild-type in two environments. **b**, Frequency distribution of the fitness of all 23,284 genotypes in each environment. Note the different scales on the *y* axes for different environments. **c**, Percentage of mutants exhibiting significant G × E. The lower left triangle shows the percentage of all genotypes whose fitness values differed significantly between the two environments compared (nominal $P < 0.05$, *t*-test), whereas the upper right triangle shows the corresponding fraction of N1 mutants.

quadratic model in describing the between-environment fitness relationships. Although the quadratic model generally outperformed the simple and piecewise linear models, the coefficient of the quadratic term was small. Also, the advantage of the quadratic model over the piecewise linear model, measured by the difference in the fraction of variance explained, was small (Supplementary Table 2). Furthermore, this advantage arose from the fact that the vast majority of genotypes were less fit than the wild-type (Fig. 2b) and that the quadratic model allows one more parameter than the piecewise linear model to describe these genotypes. When equal numbers of genotypes that were fitter and less fit than the wild-type were considered, the piecewise linear model generally performed the best (Supplementary Table 3). Because of the distinct biological meanings and evolutionary roles of deleterious and beneficial mutations, the piecewise linear model, which had equal weights for these two types of mutation in fitting, appeared more appropriate.

Predicting the FL under new environments. To evaluate how well the piecewise linear model (Fig. 3c) predicts the f_{23} of a genotype from its f_{30} estimate, we focused on 6,319 genotypes that have relatively precise experimental estimates of f_{30} and f_{23} (with ≥500 reads at T_0 and ≥1 read at T_1 in each of the 5 replicates under each of the two environments). Such restriction was necessary because of the difficulty in judging whether a prediction is good or not by comparing it with an actual measurement that is imprecise. We treated the f_{23} of a genotype estimated from the mean of five biological replicates as the observed value. The predicted and observed f_{23} values were highly correlated (Spearman's $\rho = 0.908$, Pearson's $r = 0.915$, $P < 10^{-300}$ in both tests). We define prediction error by the absolute difference between the observed and predicted f_{23}. In contrast, measurement error is the mean absolute difference between the observed f_{23} and that estimated from one biological replicate. Remarkably, the prediction error was no greater than the measurement error across the entire range of f_{30} in our data (Fig. 3d), and this pattern held for 4 of the 12 environment pairs (Supplementary Fig. 5). In addition, we quantified the prediction bias by the median difference between the predicted and observed f_{23} and found it to be minimal except when $f_{30} < 0.6$ (Fig. 3e), which was expected (see Methods). For comparison, we respectively tested a linear model with one *k* and a quadratic model (Fig. 3c). These two models had larger biases and errors when $f_{30} > 1$, but were otherwise similar in performance to the piecewise linear regression (Fig. 3d,e). These observations held in all 12 pairwise predictions from one environment to another (Supplementary Fig. 5). Another performance indicator of our prediction was the fraction of predictions that deviated significantly from the observation. Only 0.51% of the 6,319 predictions of f_{23} from f_{30} belonged to this category (false discovery rate = 0.05).

In the above exercise, the prediction model was determined by comparing the FLs respectively measured in Env_{30} and Env_{23}. In practice, we would measure the FL in Env_{30} and then predict it in Env_{23}. Because the piecewise linear model involves only two parameters (k_a and k_b), in principle we need to measure the fitness of only two genotypes, respectively fitter and less fit than the wild-type, in Env_{23} to parameterize the model. This was indeed the case, as long as f_{30} of the genotypes chosen for the fitness measurement in Env_{23} was not too close to 1 (Fig. 3f). This pattern held for most of the 12 environment-to-environment fitness predictions (Supplementary Fig. 6).

Epistasis between mutations is negatively biased. We estimated epistasis between mutations in the tRNA gene using the fitness estimates of all 207 N1 mutants and 8,101 double mutants (N2 mutants) (see Methods). In each environment, a large

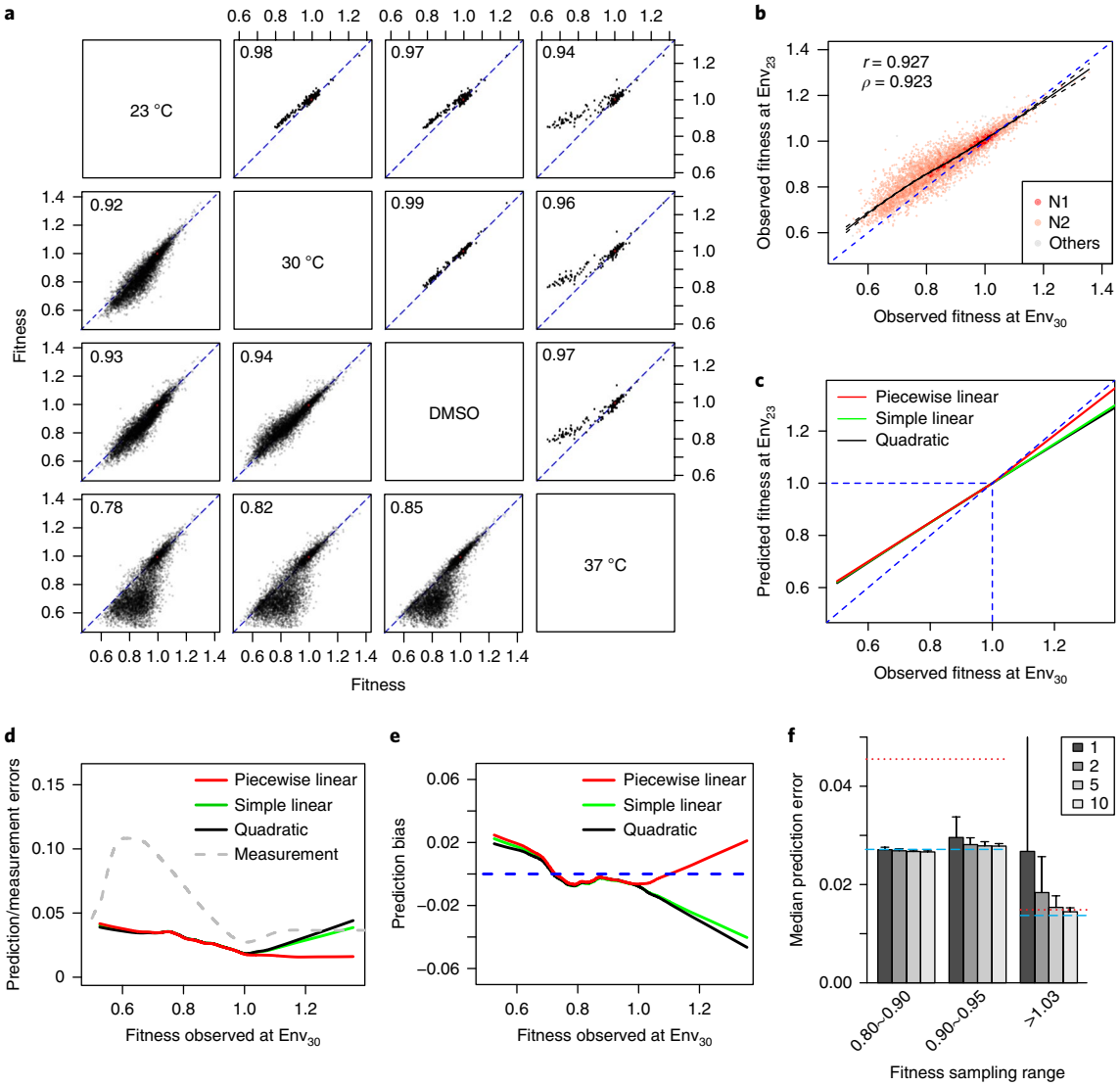

Fig. 3 | A piecewise linear model predicts the FL in one environment based on that in another. a, Fitness values from two environments were highly correlated among all mutants (lower left triangle), especially N1 mutants (upper right triangle). The Pearson's correlation coefficient is presented for each environment pair. **b**, LOESS curve (black solid curve) describing the relationship between genotype fitness in Env_{30} and Env_{23}, with 95% confidence intervals indicated (black dashed curves). Pearson's correlation (r) and Spearman's correlation (ρ) are indicated. In **a** and **b**, each dot is a genotype, and the diagonal is indicated by a blue dashed line. **c**, A piecewise linear model, simple linear model and quadratic model are respectively plotted to capture the relationship between genotype fitness in Env_{30} and Env_{23}. The blue dashed lines show $y=x$, $x=1$ and $y=1$, respectively. **d**, Prediction error and measurement error of fitness in Env_{23}. The three solid curves respectively show prediction errors under three different prediction models when fitness in Env_{23} was predicted from that in Env_{30}, whereas the grey dashed curve shows the measurement error based on one measurement in Env_{23}. **e**, Prediction bias of fitness in Env_{23}. The three solid curves respectively show prediction bias under three different models when predicting fitness in Env_{23} from that in Env_{30}. The blue dashed line shows zero bias. **f**, Measuring the fitness of only a few mutants in Env_{23} was sufficient for deriving the (piecewise) linear model used to predict the FL in Env_{23} from that in Env_{30}. When 1, 2, 5 or 10 N1 mutants (indicated by different shades of grey) chosen for fitness measurement in Env_{23} had $f_{30}<1$, the median prediction errors shown are for all mutants with $f_{30}<1$. When N1 mutants chosen for fitness measurement in Env_{23} had $f_{30}>1$, median prediction errors shown are for all mutants with $f_{30}>1$. The x axis shows the f_{30} range in which mutants were randomly picked for fitness measurement in Env_{23}. Blue dashed lines show median prediction errors when all genotypes were measured for fitness in Env_{23}. Red dotted lines show median prediction errors assuming no G×E.

fraction of mutation pairs showed significant epistasis and the epistasis was strongly biased towards negative values (Fig. 4a and Supplementary Fig. 7) except at paired sites (Supplementary Fig. 8), similar to observations in other molecules[8,12,32]. Furthermore, the average fitness of all genotypes carrying the same number (≥2) of mutations was lower than expected under the multiplicative model, again indicating pervasive negative epistasis (Fig. 4b).

G×G×E interaction is prevalent. Except for the pair of Env_{30} and Env_{DMSO}, for which mutant fitness values were similar (Fig. 2c), a substantial fraction of epistases varied between environments (Fig. 4c), revealing a prevalent G×G×E interaction. G×G×E interaction was also abundantly observed under a commonly used alternative definition of epistasis (Supplementary Fig. 9).

Given that the fitness of a genotype in one environment could be predicted from that in another environment, and that epistasis

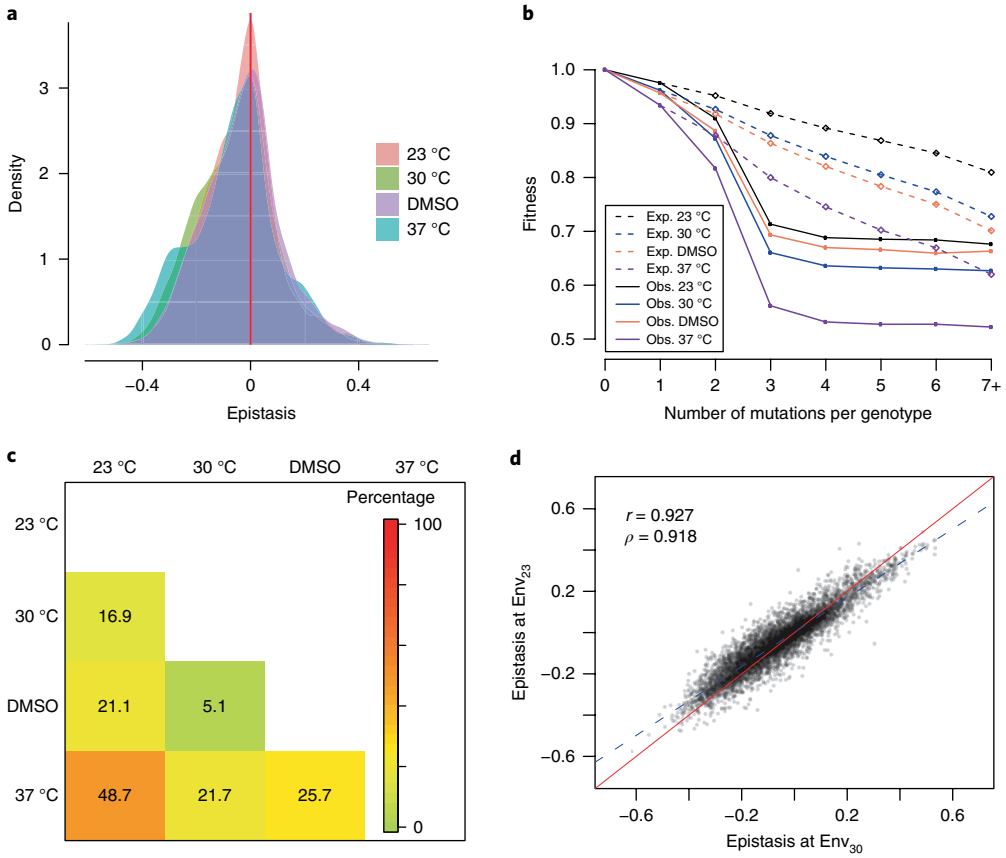

Fig. 4 | G × G × E interaction is prevalent. a, Frequency distributions of 8,101 epistases between mutations in four environments. **b**, Observed mean fitness of mutants carrying a given number of mutations (solid dots) was lower than expected under no epistasis (open diamonds) in each environment. Exp., expected; Obs., observed. **c**, Fractions of mutation pairs that exhibited significant G × G × E for each environment pair (nominal $P < 0.05$, *t*-test). **d**, Epistases measured in Env_{23} and Env_{30} were highly correlated. Pearson's correlation (r) and Spearman's correlation (ρ) are indicated. The red solid line shows the diagonal, whereas the blue dashed line shows the linear regression.

was estimated from the fitness values of three relevant genotypes, it is possible to predict epistasis in one environment from the fitness data in another environment (see Methods). Nevertheless, epistasis prediction is expected to be less precise than fitness prediction, because each epistasis prediction relies on three fitness predictions. Notwithstanding, predicting the general trend in epistasis changes upon an environmental shift may be sufficiently reliable because errors in individual epistasis predictions are random and do not alter the general trend. Our prediction of epistasis in Env_{23} from the fitness data in Env_{30} suggested a strong, positive correlation in epistasis between the two environments (Supplementary Fig. 10), which was confirmed by a comparison of epistases respectively measured in the two environments (Fig. 4d and Supplementary Fig. 11). We also predicted that epistasis holds the same direction across environments for most—albeit not all—mutation pairs (Supplementary Fig. 10), as was observed (Supplementary Table 4). We further predicted that when the mean fitness effect of mutation enlarges upon an environmental shift (for example, from Env_{30} to Env_{37}), switches from positive to negative epistasis outnumber the opposite switches, which was confirmed by our data (Supplementary Table 4). Nevertheless, none of the predicted epistasis sign switches between two environments (1) showed significant epistasis in each of the two environments concerned and (2) exhibited an epistasis sign switch, probably due to the relatively large error in predicting the epistasis of specific mutation pairs.

Discussion

In summary, we detected widespread G × E in the FLs of the yeast $tRNA^{Arg}_{CCU}$ gene across four environments, echoing accumulating reports of G × E in humans and model organisms[14,15,29,33], and supporting the importance of mapping FLs in multiple environments. Our discovery of a simple rule of G × E provides a convenient and reliable computational means to transform the FL from one environment to another with minimal additional experiments. Our observation that the fitness effect of a mutation can be linearly transformed between environments is equivalent to the statement that the ratio between the fitness effects of any two deleterious (or beneficial) mutations (say A and B) in a gene is roughly constant irrespective of the specific environment. When mutation B is a null mutation, the ratio measures the fraction of the gene's fitness contribution impacted by mutation A. The constancy of this ratio among environments leads to the interpretation that, while a gene's fitness contribution may vary among environments[2,34], a mutation in the gene influences the gene's fitness contribution by a fixed proportion that is independent of the environment. The above interpretation does not depend on the specific mechanism by which a mutation affects fitness. One critical question is whether our discovery in a yeast tRNA gene applies to other genes (especially protein-coding genes) and other organisms. To address this question, we analysed the local FLs of a segment of the yeast heat shock protein *Hsp90* gene in four environments[35] and found that the observed patterns (Supplementary Fig. 12) resembled

those in the tRNA gene. Further verifications, especially in other organisms, are needed when more multi-environment FLs become available in the future. Note that because the fitness contribution of one gene may rise while that of another may decrease upon an environmental shift, the between-environment transformation of FL is expected to be gene-specific.

We also detected widespread G×G×E interactions, which were previously reported at much smaller scales[17–22]. Because of the broad functional and evolutionary implications of epistasis, between-environment differences in epistasis cannot be ignored, especially in those rare cases where an environmental shift reverses the sign of epistasis.

In previous studies, we and others provided evidence that FLs of RNA genes under a given environment can be explained to a significant extent by RNA folding[8,9]. In the present work, our FL mapping across environments suggests that a mutation in the $tRNA^{Arg}_{CCU}$ gene influences the gene's fitness contribution by a fixed proportion that is independent of the environment. We have also explained mechanistically why the tRNA gene has a larger fitness contribution at a higher temperature, at least qualitatively. Together, these results suggest that FLs of RNA genes can be understood from a molecular mechanistic perspective and hence predicted from relevant information without exhaustive or extensive experimental mapping. Further endeavours towards this goal for both RNA and protein genes are likely to be highly rewarding.

Methods

Measuring genotype fitness in multiple environments. The chemical synthesis of the yeast $tRNA^{Arg}_{CCU}$ gene with random sequence variation has been described previously[9]. Briefly, because Integrated DNA Technologies (https://www.idtdna.com/site) could not synthesize oligonucleotides longer than 100 nucleotides that required manual mixing of nucleotides, and because there was a need for constant regions at the two ends of the oligonucleotides for the polymerase chain reaction (PCR), we could only allow 69 variable sites in the tRNA gene. Hence, the first and last two nucleotides (counting from the 5′ end) of the 72-nucleotide tRNA gene were invariant and synthesized according to the wild-type sequence. At each variable site, the probability of incorporating each of the three non-wild-type nucleotides was set at 0.01. This 'mutation' rate was chosen to maximize the fraction of variants carrying two mutations in order to study pairwise epistasis. In the pool of tRNA gene variants synthesized, the fractions of molecules with 0, 1, 2, 3, 4 and >4 mutations were expected to be 12, 26, 27, 19, 10 and 6%, respectively, while the possible numbers of variants with 0, 1, 2, 3 and 4 mutations were 1, 207, 2.1×10^4, 1.4×10^6 and 7.0×10^7, respectively. Hence, the expected genotype frequencies for given genotypes with 0, 1, 2, 3 and 4 mutations were 0.12, 1.26×10^{-3}, 1.29×10^{-5}, 1.36×10^{-7} and 1.43×10^{-9}, respectively. Previous sequencing data verified these expectations[9].

Strain construction, competition assay and library preparation were conducted as previously described[9], except that KAPA HiFi HotStart DNA Polymerase instead of AccuPrime Pfx DNA Polymerase was used for PCR amplification to further increase the accuracy of genotyping. In short, we collected over 100,000 BY4742 yeast strains carrying $tRNA^{Arg}_{CCU}$ gene variants at the native genomic location and mixed them as the starting strain pool. Cells derived from the same starting population were cultured in four separate environments and transferred every few hours to grow in log phase for ~13 generations. The exact number of generations for the whole population was computed by tracking the optical density at 660 nm (OD_{660}) over time, and the number of generations for the wild-type was then inferred from its frequency change in the population. Five parallel competitions were conducted in Env_{23} and Env_{30}, respectively, whereas three parallel competitions were conducted in Env_{DMSO} and Env_{37}, respectively. Cells were then harvested and lysed to extract DNA. Two rounds of PCR amplification were conducted to amplify the $tRNA^{Arg}_{CCU}$ gene incorporated at the correct genomic location and to add adaptors for sequencing, respectively[9]. We sequenced the common population before the competition in two technical repeats, as well as the population after each competition.

Only perfectly matched fully overlapping paired-end reads were used in estimating genotype frequencies. The change in relative genotype frequency during the competition was used to estimate the fitness of each genotype relative to the wild-type. The fitness of a genotype was calculated by averaging the fitness among biological replicates. To ensure relatively accurate fitness estimation, we focused on 23,284 genotypes with read counts ≥100 before the competition unless otherwise mentioned. The reliability of genotype fitness estimation using en masse competition followed by sequencing was previously demonstrated by comparing it with three other methods[9]. In the present study, the biological replicates allowed the assessment of estimation error.

Quantifying growth rates and fitness of selected genotypes. The growth rates of selected yeast strains were measured using a Bioscreen C optical density reader in the specific environment considered. Cells were first grown overnight until saturation, then diluted by a factor of 50 to roughly $OD_{600}=0.1$. Optical density measurements at the wide band (450–580 nm) were taken every 20 min for 48 h. The maximum growth rate was calculated following standard procedures[36]. At least two biological replications in growth measurement were performed per genotype per environment. The fitness (f) of a genotype relative to the wild-type was calculated by $2^{(R/R_0-1)}$, where R and R_0 are the maximum growth rates of the genotype and wild-type, respectively. The above formula was derived the following way. After one generation of exponential growth of a population of wild-type cells, we have $e^{R_0T}=2$, where T is the generation time of the wild-type. Similarly, we have $e^{RT}=2f$ for the genotype concerned. Combining the above two equations, we obtain $f=2^{(R/R_0-1)}$.

Quantifying G×E and G×G×E. Based on fitness estimates in multiple biological replicates, a t-test was used to examine whether the fitness of a genotype (relative to the wild-type) was significantly different between two environments at a nominal P value of 0.05, which constituted G×E. In addition to the G×E definition used in the main text (that is, the fitness of a genotype relative to the wild-type differs between environments), we also used an alternative definition of G×E that the growth rate difference between a genotype and the wild-type varies between environments[28,29].

Epistasis was defined by $\varepsilon=f_{AB}-f_Af_B$, where f_A and f_B are the fitness values of two single mutants and f_{AB} is the fitness of the corresponding double mutant. We similarly tested G×G×E by examining whether epistasis was significantly different between two environments, using a t-test at a nominal P value of 0.05. We also tested G×G×E using an alternative definition of epistasis: $\varepsilon'=\ln f_{AB}-\ln f_A-\ln f_B$ (ref. [37]).

Piecewise robust linear regression between fitness values in two environments. Local regression (LOESS) with a span of 0.5 was used to visualize the general trend in the relationship between mutant fitness measured in two environments. Using the rlm function of the MASS package in R, we conducted a piecewise robust linear regression between the fitness at one environment and that at another for genotypes with ≥500 reads at T_0 and ≥1 read at T_1 in each biological replicate of the two environments concerned. Compared with ordinary least-squares linear regression, robust linear regression reduces the potential impact of outliers. The model was fit separately for genotypes fitter than the wild-type and those less fit than the wild-type. The regression was forced to go through (1, 1) because the relative fitness was defined as 1 for the wild-type in each environment. Specifically, our regression model was

$$\begin{cases} f_2-1=k_a(f_1-1), & \text{if } f_1\le 1 \\ f_2-1=k_b(f_1-1), & \text{if } f_1>1 \end{cases}$$

where f_1 and f_2 are the fitness values of a genotype in environments 1 and 2, respectively.

In addition, we tried two alternative models to regress the fitness estimates from two environments. The first alternative model was a simple robust linear model that went through (1, 1) without separate slopes for genotypes fitter than the wild-type and those less fit than the wild-type. The second alternative model was a quadratic model that went through (1, 1). We calculated adjusted R^2 to represent the fraction of variance in fitness explainable by each model. None of the above models would be accepted if correlations between observations and predictions were weak, prediction errors were large or genotypes with significant prediction errors were numerous.

Evaluating fitness predictions. We can treat the regression line between fitness values in two environments as predictions of fitness in environment 2 from those in environment 1. Two metrics were used to evaluate these predictions. The first metric was prediction error; that is, the absolute difference between the predicted and observed fitness in environment 2. Here, the observed fitness is the mean of the measured fitness across all biological replicates. As a comparison, we computed measurement error; that is, the absolute difference between the fitness estimated from one biological replicate and that averaged across all biological replicates in environment 2. The second metric was prediction bias, which is the difference between the predicted and observed fitness in environment 2. A LOWESS (local polynomial regression) curve fitting was used to acquire a general trend of the prediction error, measurement error and prediction bias across different fitness ranges (with the smoother span = 0.2). As shown in Fig. 3e, we observed a relatively large positive bias for the prediction of f_{23} at the low fitness end ($f_{30}<0.6$). This bias was expected for the following reason. When $f_{30}<1$, f_{23} is generally higher than f_{30} (Fig. 3a). Here, because we analysed only those genotypes that had ≥1 read at T_1 in both Env_{23} and Env_{30}, f_{30} was more likely to be overestimated than f_{23},

which led to a positive prediction bias of f_{23}. In identifying outliers, fitness in Env_{23} was individually predicted from the fitness values of five biological replicates in Env_{30} using the piecewise linear model. A t-test was then used to compare the five predicted and five observed fitness values in Env_{23}, followed by a correction for multiple testing with a cut-off false discovery rate of 0.05.

To predict the FL in a new environment using the FL in an old environment and the fitness measures of a few genotypes in the new environment, we randomly picked (without replacement) various numbers of N1 mutants whose fitness values in the old environment were within designated ranges. We used the fitness measures of these mutants in both environments to construct a robust linear model, which was then used to predict the FL in the new environment. We repeated this process 1,000 times and computed the prediction bias and error, as previously mentioned, from each repeat. Note that a mutant may be used in multiple replicates.

Expected fitness under no epistasis. Under the assumption of no epistasis, the expected fitness of a genotype carrying n mutations is the product of the fitness of the n constituent N1 mutants or 0.5—whichever is larger.

Predicting epistasis in a new environment. For two N1 mutants and the corresponding double mutant, we first predicted their fitness in environment 2 from their measured fitness in environment 1. We then used the definition of epistasis to predict the epistasis between the two mutations in environment 2 from the three predicted fitness values in environment 2. This predicted epistasis in environment 2 was compared with the corresponding epistasis in environment 1.

Let the fitness of two N1 mutants and the corresponding N2 mutant be f_A, f_B and f_{AB} in environment 1 and f'_A, f'_B, and f'_{AB} in environment 2, respectively. Because the vast majority of N1 and N2 mutants are less fit than the wild-type, we assume that the formula $(f-1)=k(f-1)$ holds for all three genotypes considered here. It can be shown that the difference in epistasis between the two environments is

$$\begin{aligned}\varepsilon_2-\varepsilon_1 &= (f'_{AB}-f'_A f'_B)-(f_{AB}-f_A f_B)\\ &= -(k-1)[k(1-f_A)(1-f_B)+kf_A f_B-\varepsilon_1]\end{aligned}$$

When the mean fitness effect of mutations enlarges upon an environmental shift, $k>1$. Thus, when $\varepsilon_1<0$, which occurs for most pairs of mutations, $\varepsilon_2-\varepsilon_1$ is negative. This result explains why negative epistasis rarely becomes positive upon an environmental shift that enlarges the mean fitness effect of mutations.

Analysis of a previously published FL. For most FL mapping in the past, the exact number of generations in the competition was not reported, and hence the data cannot be used to estimate the fitness per generation. Here, we focused on a dataset that allowed estimation of fitness per generation. The dataset contains 189 mutants, representing all 20 amino acids and a stop codon at each of the nine examined positions of yeast *Hsp90* (ref. [35]). The fitness data were collected in four environments: low salinity at 30 °C, high salinity at 30 °C, low salinity at 36 °C and high salinity at 36 °C. Because no mutant showed a fitness >1.01 at low salinity at 30 °C or low salinity at 36 °C, we fit a simple linear model with a single slope k for prediction of FL in one environment from that in another. If the predicted fitness was <0.5, the lower bound value of 0.5 was assigned.

Reporting summary. Further information on experimental design is available in the Nature Research Reporting Summary linked to this article.

Code availability. The computer code is available on github.com/lichuan199010/tRNAMultiEnv.

Data availability. The National Center for Biotechnology Information accession number for the sequencing data is GSE111508. Other data are available upon request.

Received: 19 November 2017; Accepted: 27 March 2018;
Published online: 23 April 2018

References

1. De Visser, J. A. & Krug, J. Empirical fitness landscapes and the predictability of evolution. *Nat. Rev. Genet.* **15**, 480–490 (2014).
2. Qian, W., Ma, D., Xiao, C., Wang, Z. & Zhang, J. The genomic landscape and evolutionary resolution of antagonistic pleiotropy in yeast. *Cell Rep.* **2**, 1399–1410 (2012).
3. Bergland, A. O., Behrman, E. L., O'Brien, K. R., Schmidt, P. S. & Petrov, D. A. Genomic evidence of rapid and stable adaptive oscillations over seasonal time scales in *Drosophila*. *PLoS Genet.* **10**, e1004775 (2014).
4. Mitchell-Olds, T., Willis, J. H. & Goldstein, D. B. Which evolutionary processes influence natural genetic variation for phenotypic traits? *Nat. Rev. Genet.* **8**, 845–856 (2007).
5. de Vos, M. G., Dawid, A., Sunderlikova, V. & Tans, S. J. Breaking evolutionary constraint with a tradeoff ratchet. *Proc. Natl Acad. Sci. USA* **112**, 14906–14911 (2015).
6. Steinberg, B. & Ostermeier, M. Environmental changes bridge evolutionary valleys. *Sci. Adv.* **2**, e1500921 (2016).
7. Schluter, D. Ecology and the origin of species. *Trends Ecol. Evol.* **16**, 372–380 (2001).
8. Puchta, O. et al. Network of epistatic interactions within a yeast snoRNA. *Science* **352**, 840–844 (2016).
9. Li, C., Qian, W., Maclean, M. & Zhang, J. The fitness landscape of a tRNA gene. *Science* **352**, 837–840 (2016).
10. Hietpas, R. T., Jensen, J. D. & Bolon, D. N. Experimental illumination of a fitness landscape. *Proc. Natl Acad. Sci. USA* **108**, 7896–7901 (2011).
11. Findlay, G. M., Boyle, E. A., Hause, R. J., Klein, J. C. & Shendure, J. Saturation editing of genomic regions by multiplex homology-directed repair. *Nature* **513**, 120–123 (2014).
12. Bank, C., Hietpas, R. T., Jensen, J. D. & Bolon, D. N. A systematic survey of an intragenic epistatic landscape. *Mol. Biol. Evol.* **32**, 229–238 (2015).
13. Melnikov, A., Rogov, P., Wang, L., Gnirke, A. & Mikkelsen, T. S. Comprehensive mutational scanning of a kinase in vivo reveals substrate-dependent fitness landscapes. *Nucleic Acids Res.* **42**, e112 (2014).
14. Risch, N. et al. Interaction between the serotonin transporter gene (*5-HTTLPR*), stressful life events, and risk of depression: a meta-analysis. *JAMA* **301**, 2462–2471 (2009).
15. Thorgeirsson, T. E. et al. A variant associated with nicotine dependence, lung cancer and peripheral arterial disease. *Nature* **452**, 638–642 (2008).
16. Phillips, P. C. Epistasis—the essential role of gene interactions in the structure and evolution of genetic systems. *Nat. Rev. Genet.* **9**, 855–867 (2008).
17. Zhu, C. T., Ingelmo, P. & Rand, D. M. G×G×E for lifespan in *Drosophila*: mitochondrial, nuclear, and dietary interactions that modify longevity. *PLoS Genet.* **10**, e1004354 (2014).
18. Wendling, C. C., Fabritzek, A. G. & Wegner, K. M. Population-specific genotype × genotype × environment interactions in bacterial disease of early life stages of Pacific oyster larvae. *Evol. Appl.* **10**, 338–347 (2017).
19. Filteau, M. et al. Evolutionary rescue by compensatory mutations is constrained by genomic and environmental backgrounds. *Mol. Syst. Biol.* **11**, 832 (2015).
20. Lalic, J. & Elena, S. F. Epistasis between mutations is host-dependent for an RNA virus. *Biol. Lett.* **9**, 20120396 (2013).
21. De Vos, M. G., Poelwijk, F. J., Battich, N., Ndika, J. D. & Tans, S. J. Environmental dependence of genetic constraint. *PLoS Genet.* **9**, e1003580 (2013).
22. Flynn, K. M., Cooper, T. F., Moore, F. B. & Cooper, V. S. The environment affects epistatic interactions to alter the topology of an empirical fitness landscape. *PLoS Genet.* **9**, e1003426 (2013).
23. Sadowska-Bartosz, I., Paczka, A., Molon, M. & Bartosz, G. Dimethyl sulfoxide induces oxidative stress in the yeast *Saccharomyces cerevisiae*. *FEMS Yeast Res.* **13**, 820–830 (2013).
24. Bhaskaran, H., Rodriguez-Hernandez, A. & Perona, J. J. Kinetics of tRNA folding monitored by aminoacylation. *RNA* **18**, 569–580 (2012).
25. Alexandrov, A. et al. Rapid tRNA decay can result from lack of nonessential modifications. *Mol. Cell* **21**, 87–96 (2006).
26. Alexandrov, A., Grayhack, E. J. & Phizicky, E. M. tRNA m7G methyltransferase Trm8p/Trm82p: evidence linking activity to a growth phenotype and implicating Trm82p in maintaining levels of active Trm8p. *RNA* **11**, 821–830 (2005).
27. Lee, J., Vogt, C. E., McBrairty, M. & Al-Hashimi, H. M. Influence of dimethylsulfoxide on RNA structure and ligand binding. *Anal. Chem.* **85**, 9692–9698 (2013).
28. Ottman, R. Gene–environment interaction: definitions and study designs. *Prev. Med.* **25**, 764–770 (1996).
29. Wei, X. & Zhang, J. The genomic architecture of interactions between natural genetic polymorphisms and environments in yeast growth. *Genetics* **205**, 925–937 (2017).
30. Carlborg, O. et al. A global search reveals epistatic interaction between QTL for early growth in the chicken. *Genome Res.* **13**, 413–421 (2003).
31. Sackman, A. M. & Rokyta, D. R. Additive phenotypes underlie epistasis of fitness effects. *Genetics* **208**, 339–348 (2018).
32. Bershtein, S., Segal, M., Bekerman, R., Tokuriki, N. & Tawfik, D. S. Robustness–epistasis link shapes the fitness landscape of a randomly drifting protein. *Nature* **444**, 929–932 (2006).
33. Smith, E. N. & Kruglyak, L. Gene–environment interaction in yeast gene expression. *PLoS Biol.* **6**, e83 (2008).

34. Hillenmeyer, M. E. et al. The chemical genomic portrait of yeast: uncovering a phenotype for all genes. *Science* **320**, 362–365 (2008).
35. Hietpas, R. T., Bank, C., Jensen, J. D. & Bolon, D. N. A. Shifting fitness landscapes in response to altered environments. *Evolution* **67**, 3512–3522 (2013).
36. Warringer, J. et al. Trait variation in yeast is defined by population history. *PLoS Genet.* **7**, e1002111 (2011).
37. Mani, R., St Onge, R. P., Hartman, J. L. T., Giaever, G. & Roth, F. P. Defining genetic interaction. *Proc. Natl Acad. Sci. USA* **105**, 3461–3466 (2008).

Acknowledgements

We thank W.-C. Ho, W. Qian, X. Wei and J.-R. Yang for valuable comments. This work was supported by an NSF DDIG (DEB-1501788) to J.Z. and C.L., and an NIH grant (R01GM103232) to J.Z.

Author contributions

J.Z. conceived the project. C.L. and J.Z. designed the experiment. C.L. performed the experiment and analysed the data. C.L. and J.Z. wrote the paper.

Competing interests

The authors declare no competing interests.

Additional information

Supplementary information is available for this paper at https://doi.org/10.1038/s41559-018-0549-8.

Reprints and permissions information is available at www.nature.com/reprints.

Correspondence and requests for materials should be addressed to J.Z.

Publisher's note: Springer Nature remains neutral with regard to jurisdictional claims in published maps and institutional affiliations.